

Semi-flexible Additive Manufacturing Materials for Modularization Purposes

A modular assembly proposal for a foam edge-based spatial framework

Theresa Lohse¹, Liss C. Werner²

^{1,2}Technical University Berlin

¹lohsetheresa@gmx.de ²liss.c.werner@tu-berlin.de

This paper introduces a series of design and fabrication tests directed towards the use of bendable 3D printing materials in order to simplify a foam bubble-based geometry as a frame structure for modular assembly. The aspiration to reference a spittlebug's bubble cocoon in nature for a light installation in the urban context was integrated into a computational workflow conditioning light-weight, material-, and cost savings along with assembly-simplicity. Firstly, before elaborating on the project motivation and background in foam structures and applications of 3D-printed thermoplastic polyurethane (TPU) material, this paper describes the physical nature of bubble foams in its relevant aspects. Subsequently this is implemented into the parametric design process for an optimized foam structure with Grasshopper clarifying the need for flexible materials to enhance modular feasibility. Following, the additive manufacturing iterations of the digitally designed node components with TPU are presented and evaluated. Finally, after the test assembly of both components is depicted, this paper assesses the divergence between natural foams and the case study structure with respect to self-organizing behavior.

Keywords: *digital fabrication, 3D Printing, TPU flexibility, modularity, optimization*

CONTEXT

Within the context of the research project "GetHome-Safely" the experiment was to design an urban night light to be installed and tested in variable notably dark spots around the city where conventional street light glow does not reach out to. GetHomeSafely is an Innovation Activity supported by EIT Digital offering a human-centered and IoT-based network light-

ing that guides you through those dark areas. Further contexts as well as relevant requirements the project is touching upon are outlined in the following. A) Envisioned Design: The envisioned design for an irregular light-weight frame structure is inspired by and references the geometric principle of the cocoon of a spittlebug. The cocoon of a spittlebug is a bubble blob usually created at a bifurcation of leaves or

blades of grass (Figure 1a). It is made from multiple spit bubbles that agglomerate in a similar fashion as soap bubbles do, resulting in a three-dimensional 'body'. When foam bubbles are connected, three or four foam edges always meet at one intersection. These multiple intersection points are distributed according to a three-dimensional Voronoi principle (Vecchio, Redenbach, Schadelitz, 2014). The project looks at the edge condition of the spittle bug's bubble cluster and mimics its geometry (Figure 1b). B) In architecture, the Voronoi principle has mostly been employed for 2D surface division. Large scale architectural applications of materializing foam edge geometries have rarely been accomplished, yet the Beijing National Aquatics Center by Herzog & de Meuron is a successful counterexample in rigidity (Senses, 2007). In an installation scale, Thomas Saraceno's 'Entangled orbits' exhibited in the Baltimore Museum of Art 2017-2019, mimics dry foam agglomerations that simply stay balanced through tension and suspension in space [1]. C) Material: We chose light-weight materials to enable an environmentally sound design concept. Especially in 3D printing, explored material properties inform the computational design workflow and fast prototyping eliminates the risk of an insufficient completed mass production. D) 3D Printing Technology with TPU: Evaluating the use of 3D printed Thermoplastic Polyurethane material, it is striking that it has predominantly been applied in the digital fashion industry and medical research. Most designs are soles or midsoles for shoes, fine web fabrics for bendable light-weight dresses or tests for prosthetic elements in need of tensile strength. Within the do-it-yourself community, TPU is neither used in a large additive scale, instead for phone cases, costumes or replacement parts in mechanical applications.

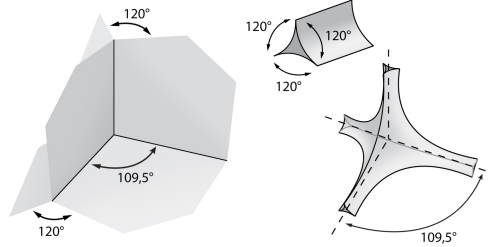


Figure 1
 a. Spittlebug's cocoon
 (www.ecoyards.com)
 b. Envisioned application of referenced structure

SPATIAL ORGANIZATION OF FOAMS

Foams are gas cells enclosed in liquid film. Foam bubbles emerge in polyhedral cells with their liquid film walls meeting in lines (edges) and intersecting at vertices (nodes). Three gas cell films always meet along one edge and four edges always intersect at one point (Figure 2a). Foams are self-organizing structures that form a static equilibrium when rather dry and under normal gravitation (Hutzler, 1997). In a biological context it is distinguished between dry foams and wet foams characterized by the parameter of liquid fraction (Waire et al, 2001). A foam is called 'dry foam' when it has very little liquid and the soap films are so thin that the liquid only exists interstitially at the foam bubbles' points of intersection (Mancini, 2005). The equilibrium of dry foam constitutes in the so-called Plateau's laws, experimentally established by the physicist Joseph Plateau and mathematician Jean Taylor in 1976. The characteristics of this state relevant for this research are: 1. Soap films, figuratively surfaces, invariably meet in threes at an angle of 120° , the Plateau border (Figure 2a). 2. This intersection of four vertices in three-dimensionality with the same angle constitutes in a tetrahedral vertex node. The vectors from a tetrahedron's geometrical centroid to the four vertices interrelate in a 109.47° or $\cos^{-1}(1/3)$ angle (Figure 2b) (Hutzler, 1997: p.22).

Figure 2
a. Plateau's equilibrium rules in dry foam polyhedral cells b. Plateau's ideal dry foam border in cross-section and perspective



Through the liquidity of the foam and its pressure being bigger than the one on the borders, the cross-section of is organized in concave triangles. Within this phenomenon of self-organization and equilibrium of dry foam it is important to keep the following in mind: Since the gas cells are of different size have varying edge lengths, the bubble edges are no straight two-point lines in the equilibrium state geometrically defined by Plateau. The edges arbitrarily adapt their route in space to form the perfect tetrahedral vertex intersection. For this experiment, the foam structure is broken down to the foam cell edges and their intersections, leaving the film surfaces unconsidered.

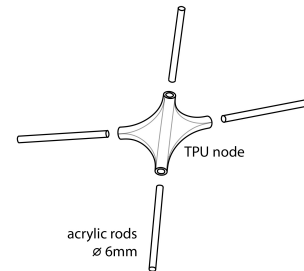
Figure 3
Modularity through two components: nodes and rods

MODULARITY AND VARIETY

Structurally mimicking the variety of 3D Voronoi edge intersection nodes spawns a difficulty in assembly due to every single node being bespoke. To minimize planning, production and assembly complexity as well as costs, modularity in the build-up is inevitable. We developed a system with two generic modular components (Figure 3) that are nodes and linear connecting edge elements, in a number of variations. They are defined as follows: The rod embodies the foam cell edge up unto the intersection point. The node is the entire joint that builds around the intersection point of the cell edges in a three-dimensional environment. Its center point is the exact intersection point of the cell edges. This encases the rod ends in a shaft at a fraction of their length.

The node component design is elaborated in the following chapter. The experiment is set up to emphasize on modularization of the bubble foam ge-

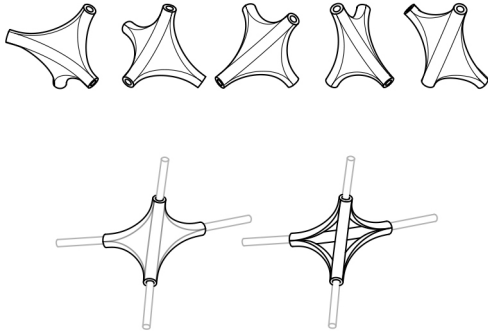
ometric principle: firstly, through computational alterations and secondly, through physical material properties and the exploitation of material behavior. Through a combination of geometry and material properties we are achieving semi-flexibility allowing the angles between the foam edges to further adjust to the overall network. The modularization entails a limited number of different types of nodes (Figure 4), limited angles between the rod shafts as well as a progressively limited length of the hollow shafts. It also necessitates an incremental limit to the rod lengths representing the distance between the nodes' center points. It is apparent that various configurations of the nodes and rod lengths reveal a visually varied pattern from a foam edge distribution and consequently show a different structural behavior.



COMPUTATIONAL FORM DETERMINATION AND GEOMETRY

Firstly, a digital twin of a representative dark corner in the city is modeled in 3D and within boundaries randomly populated with points in Grasshopper. This allows for two options for the subsequent form finding step: a) The points serve as the input points for a Grasshopper 3D Voronoi component. The angles and distances of the edges are modified thereupon. b) The points are connected by curves and determine the angles and distances of the curves. This represents a manual build-up of the structure. Here, we tested option a) to stay close to the principle of a foam geometry. The following experiment description clarifies that the initially set amount of points

neither determines the density of the frame structure nor the amount of nodes. The cell surfaces generated by the 3D Voronoi component are left unconsidered and the cell edges are deconstructed and organized as curves with intersection points in data lists. Aforementioned, in an equilibrated dry foam the cell edges do not represent straight lines intersecting in a tetrahedral angle. In contrast, the computationally generated 3D Voronoi frame by Grasshopper sets up straight lines as A to B vectors, since the system cannot undertake and simulate the chemically motivated self-organization. The resulting angles between each four cell edge curves intersecting vary approximately between 60° and 140° as a general rule. While constraining the angle parameter between these edge curves, it is essential to distribute between direct and indirect neighboring curves at the vertex. The domain limiting the angle only applies to the two directly adjacent edges, not the opposite one. What are we setting the domain to 85° to 130° considering the tetrahedral state of all angles at 109,47° (Figure 4).



The subsequent operation is setting a restriction to the foam bubble edge length. This domain defining the length of the cell edge curves entails purging curves outside of it. Since the length of each edge curve is determined by its end and start point, any change of length in order to meet the require-

ments would again affect the angles and the entire point cloud. To relax these, the points have to allow for movement through the angle adjustments. As for the prototype, the domain is set between 20cm and 50cm for the acrylic rods. The optimization of the edge curves automatically sets the construction axes of the nodes. They are further parametrically designed by a script in Python for Grasshopper to smoothly connect the shafts for the rods around the center point (Figure 4 and 5). The node shafts are computationally restricted in length according to the overall edge curve length. This parameter will have a notable impact on the overall flexibility of the entire node.

The further the semi-flexible filament encases the acrylic rod the more flexibility is given since TPU bends easier than the acrylic resin. To be proportionally dimensioned to the acrylic rods and speed up the production process for testing, the maximum span of the tetrahedron based joint will be approximately 8cm. Computational form finding was exploited to generate various exemplary nodes rather than defining a typical node and the Grasshopper optimization does not output a certain number of different types. Choosing a few nodes from the system for production ensures a final structure built in irregularity. Regularity cannot be expected from our single-rule modular build-up.

ADDITIVE MANUFACTURING OF THE FLEXIBLE NODES

There is a variety of technologies in additive manufacturing that can be attributed to four different categories by the material used: photopolymer-curing, granular, lamination and fused deposition modeling (Fastermann 2016); and each one entails specific fabrication attributes, opportunities but also constraints. For this experiment fused deposition modeling FDM technology or also called fused filament fabrication FFF is performed with an Ultimaker 3, where the material filament is heated in the print core, expelled through a brass nozzle and deposited in layers to build up the model.

Figure 4
Joint variations
generated by
Grasshopper

Figure 5
Smoothened
connections with
and without skin
(skeleton)

Printing Iteration	Unit	recommended by Ultimaker website	P1	P2	P3	P4	P5
			normal 0.15mm	fine 0.1mm	normal 0.15mm	normal 0.15mm	normal 0.15mm
Layer Height	mm		0.15	0.1	0.15	0.15	0.18
Initial Layer Height	mm	0.27	0.15	0.15	0.27	0.27	0.27
Line Width	mm		0.38	0.38	0.38	0.38	0.38
Shell: Wall Thickness	mm	0.76	0.7	0.7	0.76	0.5	0.7
Shell: Top Thickness	mm					0.66	0.7
Shell: Bottom Thickness	mm					0.7	0.7
Infill: Infill Density	%	10	15	15	18	20	20
Infill: Infill Pattern			Cross 3D	Cross 3D	Cross 3D	Concentric	Concentric
Printing Temperature	°C		225	225	225	225	225
Build Plate Temperature	°C		60	60	60	60	60
Print Speed	mm/s		25	25	25	25	25
Retraction Speed	mm/s		off	off	35	35	35
Retraction Travel	mm		off	off	0.76	0.76	0.76
Support Overhang Angle	degree				45	45	45
Support Density	degree				40	20	20
Support Pattern					Triangles	Triangles	Triangles
Printed result			failed	failed	not flexible	ripped walls	thin walls

Figure 7
Modified Ultimaker 3 settings in the prototyping phase

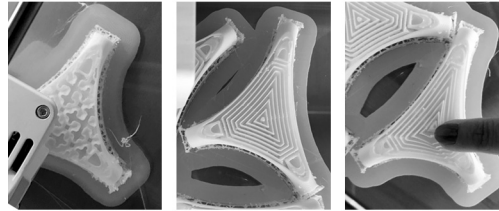


Figure 8
a. Cross 3D infill pattern of 3D printed flexible node b. Concentric infill pattern of 3D printed flexible node c. Concentric infill pattern pushed for flexibility test ©TheresaLohse

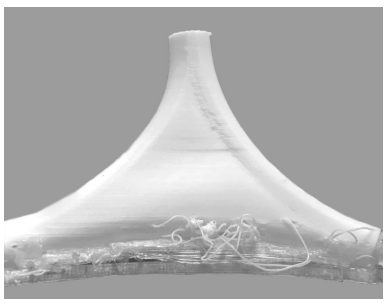


Figure 9
Outer wall thickness showing rupture ©TheresaLohse

However, due to the positioning of the geometry on the build plate of the 3D printer, the direction of pliability allowed by the concentric infill varies for each shaft since the infill is technically set up on two axes only. As an alternative pliability test, the skin and infill were removed and only the geometry skeleton (Figure 5) was printed with a diameter of about 6mm. The print failed and demonstrated remarkable stability deficits. As summarized in the print parameter table (Figure 7), prints progressively turned out more adequately. However, there is a visible inconsistency and rupture (Figure 9) in layer bonding and adhesion in the outer wall build-up. This showed to be a risk especially in assembly with the acrylic rods that channel the tension force more concentrated on the axes of the node. As a conclusion for the 3D printing process, TPU solely as a material did not prove sufficient flexibility for our application, instead it is a mixture of interior and exterior geometry setup of the node and the semi-flexible material. The wall thickness and density as well as the retraction speed of the nozzle had to be carefully adjusted to reach satisfactory results.

Figure 10
TPU node flexibility
in structure
assembly
©TheresaLohse

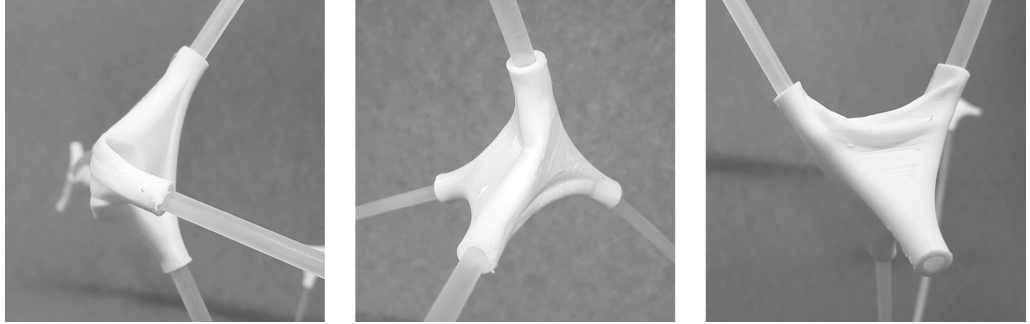
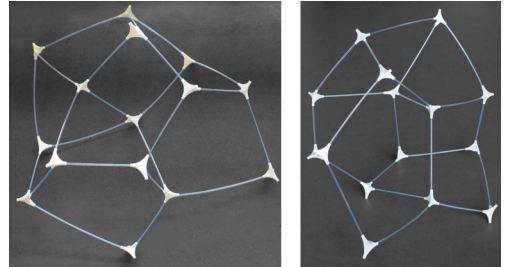


Figure 11
Test assembly of
both modules
©TheresaLohse

ASSEMBLY AND FLEXIBILITY TEST - DISCOVERIES

This research targeted generating an irregular modular node and rod structure referencing bubble foam in a simple assembly for anyone in any place. The two modules are stuck together in a simple fashion without additional adhesive. The rods were manually cut to 4 different lengths of 20cm, 25cm, 30cm and 35cm to reduce production complexity. During assembly, it was discovered that we are dealing with a divergent self-organization of the structure contrary to the dry foam in equilibrium. We learned that in a dry foam, the 'soft' cell edges "as a network of narrow [liquid] channels [filled with air] with a triangular cross-section" (Hutzler, 1997: p.22) adapt to the node organizing the four intersecting edges in a tetrahedral manner. The cell edges undertake the spatial adaptation resulting in the tetrahedral joints. As for our assembly, the chosen acrylic rods of 6mm diameter are slightly flexible only along the center axis attributed to their shape which is dissimilar to the isotropic behavior of the liquid cell edges in foam. The stress caused by the self-organization unevenly splits up between the node and rod as they do not consist of the same cellular build-up. Nevertheless, the TPU node underlies most necessary bending in our structure whereas the acrylic rods stay fairly 'straight' (Figure 10).



Practically, an inversion of the dry foam self-organization principle exists: Node: The nodes are particularly designed closely to a fourfold junction of a Plateau borders to enable irregular adaptation to deformations. Rods: The material choice allows only minor adaption through bending. Since the TPU node complies to stress first, the rod is not challenged in equal measure. The deformation of both the TPU nodes and the acrylic rods is unpredictable and will be different in each modular assembly variation. As mentioned, the semi-flexible joints show anisotropic bending behavior rooted in the additive manufacturing set-up (Figure 11). This combination of two semi-flexible materials induces general bending rigidity in the assembled structure. However, the structure does not structurally function like a conventional space frame because it is neither regular nor based on a rigidity matrix. Despite the necessity to analyze the structural soundness of the assembled structure, its overall stiffness and compression stresses are perceivable. In order to conduct a reli-

able structural analysis, the node has to be regular and the assembly rules for a repetition of certain nodes have to be established and complied with.

CONCLUSION

The objective was to challenge adaption through material behavior in order to simplify the variations for production rather than exemplifying all possible node variations. The tested prototype delivered convincing results to understand the degree of flexibility in the node for a modular and unplanned three-dimensional foam node and rod structure. The visual appearance referencing a foam agglomeration is satisfactory if the number of foam edge rods do not fall below four and exceed 7. Yet, the print settings regarding layer height, line width and outer wall thickness cannot be easily scaled up proportionally to the model size. Firstly, the extruding nozzle diameter affects the limitation of the line width, albeit it is recommended to stay as close as possible to the 0.4mm nozzle width for successful prints. Secondly, the overall size of the printer is limited to 197 x 215 x 300 mm and tied to the nozzle-governed layer resolution hence, a different 3D printer ought to be used. The experiment also does not reflect upon a deep structural analysis and simulation undertaken by digital structural analysis tools. To a degree, the assembled structure stabilizes similar to the self-stabilization of a foam through self-organization of the bubbles respectively the nodes and rods. The prototype did not show a structural deficit caused by its dead load, yet when extending the structure in this scale by nodes and rods, extra stabilization might be necessary. Conclusively, the prototyping endeavors with semi-flexible material helped to reveal the impact on larger scaled constructions and installations employing an adjustable, spatial foam cell edge-led node and rod system, as very promising due to the remarkably simple and fast assembly.

ACKNOWLEDGEMENTS

We wish to thank Professor Raoul Bunschoten, CHORA Conscious City, chair of the department for

Sustainable Urban Planning and Design, Institute of Architecture at Technical University of Berlin for supporting the research conducted. Research was co-funded by the European Union, H2020, EIT Digital 2019, Action Line 'Digital Cities', activity number 19053.

REFERENCES

- Chua, CK and Leong, KF 2017, *3D Printing And Additive Manufacturing - Fifth Edition of Rapid Prototyping: Principles and Applications*, World Scientific Publishing Co. Pte. Ltd., Singapore
- Cunningham Boyce, M and Qi, J 2005, 'Stress-strain Behavior of Thermoplastic Polyurethanes', *Mechanics of Materials*, 73 (8), pp. 817-839
- Fasterman, P 2016, *3D Drucken - Wie die generative Fertigungstechnik funktioniert*, Springer Verlag
- Hohimer, C, Christ, J, Aliheidari, N, Mo, C and Ameli, A 2017 '3D printed thermoplastic polyurethane with isotropic material properties', *SPIE Proceedings Vol. 10165, Behaviour and Mechanics of Multifunctional and Composites 2017*
- Hutzler, S 1997, *The Physics of Foam*, Ph.D. Thesis, University of Dublin
- Kontiza, I., Spathi, T and Bedarf, P 2018 'Spatial Graded Patterns - A case study for large-scale differentiated space frame structures utilizing high-speed 3D-printed joints', *Proceedings of the 36th International Conference on Education and Research in Computer Aided Architectural Design in Europe*, Łódź, Poland
- Mancini, M 2005, *Structure and evolution of soap-like foams*, Ph.D. Thesis, Université de Cergy-Pontoise
- Senses, N 2007, *Foam Structures: A Comparative Structural Efficiency Analysis Based on the Building Case "Watercube"*, Master's Thesis, TU Vienna
- Vecchio, I, Redenbach, C and Schadelitz, K 2014, 'Angles in Languerre tessellation models for solid foams', *Computational Material Science*, 83, pp. 171-184
- Weaire, D, Verbist, G, Cox, SJ and Hutzler, S 2001 'Pleary Lecture: Frontiers of the Physics of Foams', *Microgravity Research and Applications in Physical Sciences and Biotechnology, Proceedings of the First International Symposium held 10-15 September, 2000 in Sorrento, Italy. Edited by O. Minster and B. Schürmann. European Space Agency, ESA SP-454*
- [1] <https://artbma.org/exhibitions/tomas-saraceno>
- [2] <https://ultimaker.com/materials/tpu-95a>
- [3] <https://ultimaker.com/materials/pva>